Characterisation of syndiotactic polystyrene/ carbon nanofiber composites through X-ray diffraction using adaptive neuro-fuzzy interference system and artificial neural network

S. Bose [a,*], D. Shome [b], C.K. Das [a]
[a] Materials Science Centre, Indian Institute of Technology, Kharagpur – 721302, India
[b] Department of Industrial Engineering and Management,
Indian Institute of Technology, Kharagpur – 721302, India
* Corresponding author: E-mail address: bose_saswata@yahoo.co.in

ABSTRACT

Purpose: The purpose of the paper is to characterize of syndiotactic polystyrene/carbon nanofiber composites through X-ray diffraction using adaptive neuro-fuzzy interference system and artificial neural network. Owing to their interesting mechanical, electrical and thermal properties, syndiotactic polystyrene (s-PS)/carbon nanofiber (CNF) composites have gained adequate importance in the scientific and industrial communities and as a result, characterization of s-PS/ CNF is an issue of major interest to the researchers.

Design/methodology/approach: In the present paper, two quantitative models, based on adaptive neuro-fuzzy interference system (ANFIS) and artificial neural network (ANN), are developed and compared with a goal of accurately predicting the intensity values from the scattering angle values in X-ray Diffraction (XRD) of syndiotactic polystyrene (s-PS)/carbon nanofiber (CNF) composites.

Findings: Results demonstrate that both the proposed models are highly effective in estimating intensity from scattering angle. However, more accurate results are obtained with the ANFIS model as compared to the ANN model.

Research limitations/implications: The results of the investigations carried out in this study is suggestive of the fact that both ANFIS and ANN can be used quite effectively for prediction of intensity from scattering angle values in XRD of s-PS/ CNF composites.

Originality/value: The proposed ANFIS and ANN model-predicted intensity values are in very good agreement with the experimental intensity values. However, it is seen that, irrespective of the type of composite sample, the proposed ANFIS models outperform the proposed ANN models in terms of prediction accuracy.

Keywords: Syndiotactic polystyrene; Carbon Nanofiber; X-ray diffraction; Artificial Neural Network; Adaptive neuro-fuzzy interference system

Reference to this paper should be given in the following way:

S. Bose, D. Shome, C.K. Das, Characterisation of syndiotactic polystyrene/carbon nanofiber composites through X-ray diffraction using adaptive neuro-fuzzy interference system and artificial neural network, Archives of Computational Materials Science and Surface Engineering 1/4 (2009) 197-204.

ENGINEERING MATERIALS

1. Introduction

Adequate importance in the scientific and industrial communities have been gained by Syndiotactic polystyrene (s-PS)/carbon nanofiber (CNF) composites owing to their interesting mechanical, electrical and thermal properties. The interesting mechanical, electrical and thermal properties of the above-mentioned composites are mainly because of their high aspect ratio [10,11]. For a high performance nano-filler/polymer composites, a homogeneous dispersion of the fillers in the polymer matrices as well as a strong interface interaction between the polymer and the fillers, are two very important criteria. In order to develop a strong interface interaction between the polymer and the fillers, appropriate particle size/crystallite size of dispersed phase must be achieved [10,11], which in turn can be assessed from the peak intensity. Moreover, stronger nucleating effect of fibers is dependent on the concentration of CNF's loadings into the polymer matrix [7] and this concentration can also be estimated from the peak intensity. As a result, characterization (XRD) of Syndiotactic polystyrene (s-PS)/carbon nanofiber (CNF) with a view of assessing the peak intensity is an issue of major concern.

Several studies [7,10,11] on characterization of Syndiotactic polystyrene (s-PS)/carbon nanofiber (CNF) composites through X-ray diffraction (XRD) have been reported in the literature. However, the potential of a quantitative model in estimating peak intensity in XRD of Syndiotactic polystyrene (s-PS)/carbon nanofiber (CNF) composites still remains unexplored. This inadequacy calls for further research from the viewpoint of proposing accurate quantitative model(s) for accomplishing accurate estimation of peak intensity in XRD of Syndiotactic polystyrene (s-PS)/carbon nanofiber (CNF) composites.

In this study, X-ray diffraction (XRD) of four types of Syndiotactic polystyrene (s-PS)/carbon nanofiber (CNF) composite samples (having different composition) are conducted and for each sample, an ANFIS [12,13,16-18] as well as an ANN model [5,9,15] are proposed for prediction of the intensity values from scattering angle values. Investigations carried out reveal that, for each of the composite samples, relatively more accurate results are obtained through the corresponding ANFIS model.

2. Experimentation

This section presents detailed discussions about various aspects pertaining to experimentation carried out in this study.

2.1. Materials

The CNFs used in the current study are designated as CNF-100, and are from Carbon Nano-material Technology Co. Ltd., Korea. The diameter, length and aspect ratio were 40–140 nm, 2–10μm and ˜100, respectively. Syndiotactic polystyrene used in this study was obtained from PolyOne Germany. The glass transition temperature (Tg) and the crystalline melting temperature (Tm) of s-PS are 95-100^{0}C and 270-280^{0}C, respectively.

2.2. Experimental procedure

In this section, the procedure followed for conducting experiments in this study is described in details.

Preparation of s-PS/CNF Composite

Before the start of mixing, the s-PS pellets were dried under vacuum at 80^{0}C for at least 12 h and CNF-100 were dried under vacuum at 300^{0}C for the same time. s-PS /CNF composites were prepared in a Sigma high temperature internal mixer equipped with two counter-rotating Sigma type rotors at 320^{0}C, with a speed of 100 rpm and a mixing time of 5-8 minutes. The procedure was as follows: firstly the polymer was melted. After that carbon nanofibers were incorporated into the molten polymer matrix. In this typical experiment 100 phr of s-PS pellet were mixed with 2, 4 or 6 phr of CNFs.

The neat s-PS, s-PS /CNFs samples were dried at 80 ^{0}C for 12 h and then the obtained composites were compression molded under a pressure of about 15 MPa at 300^{0}C for 10 min. The samples were allowed to cool to room temperature under the same pressure at the rate of 2 ^{0}C/min. Formulations of the s-PS/CNF composites are shown in Table 1.

Table 1.
Formulation of s-PS/CNF composites

Sample Code	s-PS (phr)	CNF (phr)
P	100	-
A	100	2
B	100	4
X	100	6

Characterization using X-Ray Diffraction (XRD)

X-Ray Diffraction was studied using PW 1840 X-ray diffractometer with Cu-Kα -targets at 2mm slits at a scanning rate of 0.050 2θ/sec., chart speed 10 mm/2θ, range 5000c/s, applying 40 kV, 20 mA, to get the idea of the relative crystallinity of the composites. The crystalline and amorphous portion was determined by arbitrary units. The degree of crystallinity χ_c was measured using the following relationship:

$$\chi_c = I_a/(I_a+I_c).$$

where, I_a and I_c are the integrated intensity of the crystalline and amorphous region respectively, where, the crystallite sizes (P) and the interplaner distance (d) were calculated as follows:

$$P = K \lambda/\beta \cos \theta.$$
$$d = \lambda/2 \sin \theta$$

where, β is the half height width (in radian) of the crystalline peak and λ is the wave length of the X-Ray radiation (1.548 for Cu) and k is the Scehrrer constant taken as 0.9.

3. Modelling of intensity in XRD

This section carries out detailed discussions about the ANFIS and the ANN models proposed in this paper for prediction of intensity in XRD of s-PS/CNF composites.

3.1. Proposed ANFIS models

In this study, a total of four five-layer ANFIS models are developed for the purpose of predicting intensity from scattering angle. Figure 1 exhibit the general architecture of the ANFIS models used in this study. An ANFIS model is highly effective in terms of prediction accuracy [16]. The input parameter of each of the ANFIS models is scattering angle (S) and the output parameter is intensity. Various important aspects pertaining to the ANFIS models developed in this paper and their training are given in Table 2. For each of the ANFIS models developed in this study, the number of rules to be used in the ANFIS model, the number of membership functions to be assigned to each input variable of the concerned ANFIS model, and the number of training epochs required for training the concerned ANFIS model, are decided based on a trial and error approach. A first order Takagi-Sugeno-Kang fuzzy model [19] is used for each of the ANFIS developed in this study because it is computationally more effective than other fuzzy models, such as, Mamdani and Tsukamoto models [20]. In this study, generalized bell- shaped membership functions are used for specifying fuzzy sets for the concerned ANFIS models due to their smoothness and concise notation [20]. A hybrid learning algorithm [17] is adopted for training each of the ANFIS models because it has the capability of increasing the speed of the ANFIS's learning process [16]. During training, the value of initial step size is fixed at 0.01 because the value of initial step size does not adversely affect the performance of a trained ANFIS model unless it is too high [16].
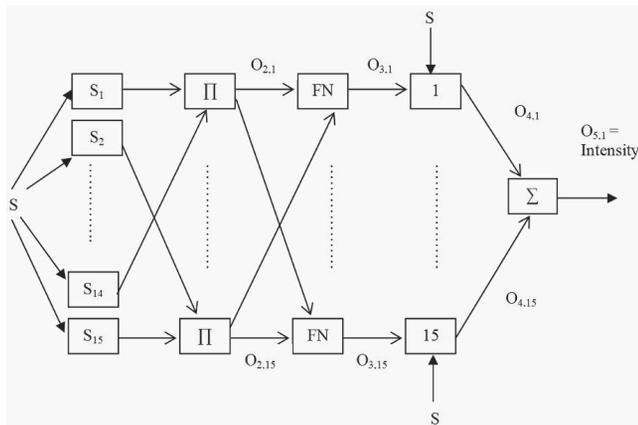
Fig. 1. General Architecture of ANFIS Model

The convergence of error during training process of the proposed ANFIS are shown in Figures 2-5. The ANFIS models for sample A, sample B, sample X and sample P are trained with 1000, 1000, 1000 and 800 data sets respectively and validated (tested) with 24, 23, 21, 20 data sets respectively. The mean % errors (furnished in Table 3) of the ANFIS models is determined using the following expression:

$$\text{Mean Absolute Error} = \frac{1}{n} \sum_{k=1}^{n} \left[\left| 100 - \left(\frac{p_k \times 100}{q_k} \right) \right| \right] \%$$

where, q_k represent the experimental intensity values and p_k represent those predicted by the trained ANFIS model and n represents the total number of datasets.

Table 2.
Details of some important aspects associated with the ANFIS Model

Number of input variables:	1
Number of output variables:	1
Number of network layers:	5
Number of fuzzy sets for each input parameter:	15
Initial step size:	0.01
Number of rules:	15
ANFIS model type:	First-order Takagi-Sugeno-Kang model
Number of training iterations:	500
Input membership function type:	Generalized Bell-Shaped
Output membership function type:	Linear
ANFIS Training method:	Hybrid (Gradient descent method for the antecedent parameters and least squares estimation method for the consequent parameters)
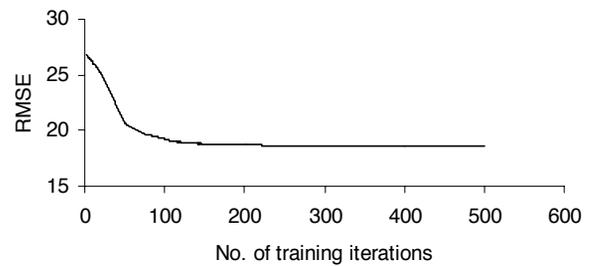
Fig. 2. Convergence of error during training of ANFIS for sample A
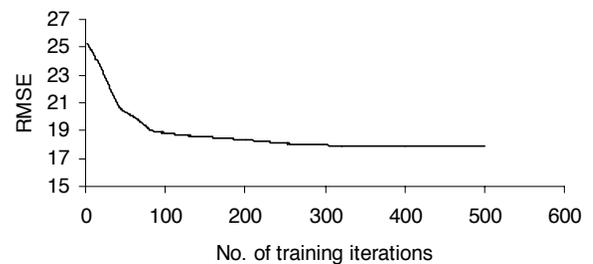
Fig. 3. Convergence of error during training of ANFIS for sample B
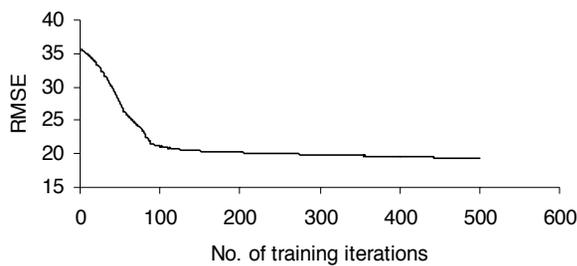
Fig. 4. Convergence of error during training of ANFIS for sample X
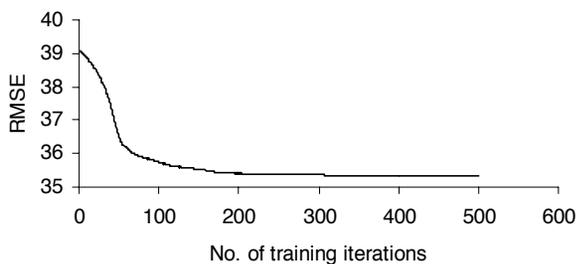
Fig. 5. Convergence of error during training of ANFIS for sample P

Table 3.
Comparison between the proposed ANFIS and ANN Models

Sample	Model	Mean % Error (training)	Mean % Error (test)
A	ANFIS	5.02	3.53
	ANN	4.93	4.84
B	ANFIS	5.39	2.97
	ANN	5.30	4.58
X	ANFIS	5.07	3.22
	ANN	2.50	5.83
P	ANFIS	2.47	2.35
	ANN	4.69	2.78

3.2. Proposed ANN models

In this study, a total of four three-layer neural networks are developed for the purpose of predicting intensity from scattering angle. The neural networks used for predicting intensity from scattering angle in case of samples A, B, X and P have 39, 39, 70 and 28 hidden nodes respectively. Figure 6 exhibit the general architecture of the ANN models used in this study. There is one input node and one output node representing scattering angle and intensity respectively. The basic requirement for any neural network to have a good capacity of predicting the output from unseen input(s) (input(s) not presented to the concerned network during its training) is the presence of the minimum number of hidden nodes required for the above-mentioned purpose [14]. Each of the neural networks developed (as mentioned above) is trained through Bayesian Regularization algorithm [2-4,6,8,14] to increase the network's efficiency of accurately predicting unseen

data. The neural networks for the composite ssamples mentioned above are trained and validated with the same datasets as used for training and validation of the ANFIS models. 500 training iterations are used for training each of the ANN models developed in this study. Before training, the input parameter as well as the output parameter are normalized in the range of 0 to 1. Bayesian regularization is based on the assumption that the true underlying function between input–output pairs should be smooth and the desired smoothness can be achieved by keeping network weights small and well distributed within the network [14]. The performance of a neural network in Bayesian Regularization algorithm is estimated using the following relation [3,4]:

$F = \alpha(SSE) + \beta(SSW)$

where,

F = Performance Index,

$SSE = \text{Sum of error squares} = \sum_{z=1}^{n}\left(y_z^a - y_z^p\right)^2$,

for z = 1, 2,……..,n

where, n = the total number of data sets used for training and y_z^a and y_z^p represent the actual and predicted outputs respectively.

$$SSW = \sum_{i,j,k}\left(w_{ij}\right)^2 + \sum_{r,i}\left(v_{jk}\right)^2 + \sum_{i}\left(b_j\right)^2 + \sum_{r}\left(b_k\right)^2$$

for i=1,2…..,q; j=1,2……,r; k=1,2,……,s;
where, q=number of input nodes, r=number of hidden nodes, s=number of output nodes.
α, β are regularization parameters.
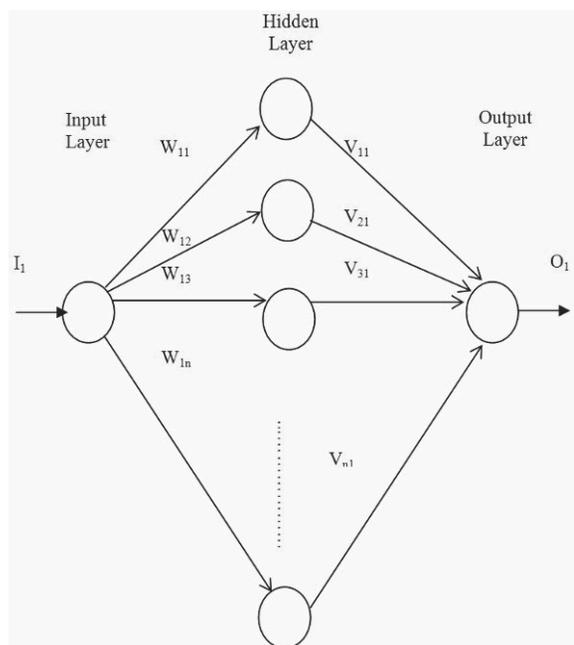
Fig. 6. General Architecture of ANN Model I_1 is the input parameter (O_1 is the output parameter, V_{11}, V_{12},……………,V_{n1} are the weights of synapses connecting hidden neurons and output neurons, W_{11}, W_{12},……………,W_{1n} are the weights of synapses connecting input neurons and hidden neurons, n = Number of hidden nodes

The values of mean % errors (furnished in Table 3) are calculated as follows:

$$\text{Mean \% error} = \frac{1}{n}\sum_{z=1}^{n}\left[\left[100 - \left(\frac{y_z^p \times 100}{y_z^a}\right)\right]\right], \text{ for } z = 1, 2, \ldots\ldots, n$$

The values of SSE (training), SSW, NOEP (number of effective parameters) and mean % error (test), as obtained from the training of the ANNs of the present study, are shown in Tables 4-7. From Table 4, it is observed that, the values of, SSE, SSW, NOEP and mean % error (test) for model no. 12 are 0.36, 59475, 62.2 and 4.84 respectively which are roughly consistent even if the number of hidden nodes increases. Similarly, from Table 5, it is observed that, the values of, SSE, SSW, NOEP and mean % error (test) for model no. 7 are 0.33, 56354, 63.7 and 4.58 respectively which are roughly consistent even if the number of hidden nodes increases. Again Table 6 shows that, the values of SSE, SSW, NOEP and mean % error (test) for model no. 4 are 0.089, 21316, 43.9 and 2.78 respectively, which are roughly consistent no matter whatever be the total number of hidden nodes. From Table 7, it is observed that, the values of, SSE, SSW, NOEP and mean % error (test) for model no. 8 are 0.254, 352799, 117.3 and 5.73 respectively, which are approximately same even if the number of hidden nodes increases. The results presented in Tables 4 -7 act as a guideline for selection of the optimal-sized neural network and based on these results ANN model no. 12, 7, 4 and 8 are selected for predicting intensity from scattering angle in case of sample A, B, P and X respectively.

4. Results and discussions

This section discusses in details the behaviour of the lattice parameters observed from the XRD results. A discussion on the training and validation results of the proposed ANFIS and ANN models are also presented followed by a comparison between those models.

4.1. Investigation of lattice parameters through XRD

The result obtained from X-ray diffraction spectra of s-PS/CNF composites is represented in Figure 7 and the values are given in Table 3. Considering the maximum single peak value ($2\theta = 20.35°$) of the s-PS/CNF composites, the features like crystallite size, and interlayer spacing are calculated. The value of crystallite size of pure s-PS, sample A, sample B, and sample X are 28.45 Å ($d \sim 4.45$), 37.1Å ($d \sim 4.38$), 47.7Å ($d \sim 4.40$), and 48.2 Å ($d \sim 4.41$) respectively. The decrease in the spacing for sample A, as compared to pure s-PS, explains that the composite structure is more compact. But the interlayer spacing increases with an increase in the CNFs loading which indicates the intercalation of s-PS into carbon nanofibers. In case of sample X, the crystallite size does not change appreciably as compared to sample B, suggesting that almost enough carbon nanofibers are

present in sample B to provide sufficient surface area for the crystal to grow. The increase in the crystallite size matches with the heteronucleation effect of the carbon nanofiber.

Table 4.
Training Results for different ANN Architectures for sample A

ANN model no.	No. of Hidden layers	SSE	SSW	NOEP	TNOEP	Mean % Error (test)
1	20	0.39	20237.8	37.3	61	4.48
2	21	0.39	21069	41.2	64	4.37
3	22	0.39	22130	41.9	67	4.34
4	23	0.39	62672	51.9	70	4.95
5	25	0.38	34054.6	50.4	76	4.81
6	27	0.39	21257.1	41.5	82	4.82
7	30	0.39	23154	43.8	91	4.40
8	32	0.37	40600.1	55.6	97	4.91
9	36	0.37	48490	58.6	109	4.51
10	37	0.36	86617	66.9	112	4.46
11	38	0.36	71535	64.2	115	3.98
12	39	0.36	59475	62.2	118	4.84
13	41	0.36	61162.4	63.1	124	3.84
14	42	0.36	60768	62.5	127	4.92
15	43	0.36	62069	63.4	130	4.79
16	44	0.36	58796.6	62.4	133	4.94
17	45	0.36	60626	63.5	136	4.93
18	46	0.36	61759	63.4	139	4.78
19	47	0.36	60170	65.1	142	4.92

Table 5.
Training Results for different ANN Architectures of sample B

ANN model no.	No. of Hideen layers	SSE	SSW	NOEP	TNOEP	Mean % Error
1	25	0.34	44280	52.8	76	4.55
2	29	0.34	50361	54.5	86	4.52
3	33	0.34	71529	59.9	100	4.53
4	36	0.33	63589	63.7	109	4.53
5	37	0.33	50864	59.4	112	4.55
6	38	0.33	49775	59.6	115	4.45
7	39	0.33	56354	63.7	118	4.58
8	40	0.33	57190	64.1	121	4.49
9	41	0.33	56122	64.3	124	4.52
10	42	0.33	57377	65	127	4.51
11	43	0.33	57331	64.1	130	4.51

Table 6.
Training Results for different ANN Architectures of sample P

ANN model no.	No. of Hideen layers	SSE	SSW	NOEP	TNOEP	Mean % Error (test)
1	20	0.11	6941	28.01	61	2.79
2	25	0.09	17014	41.04	76	2.83
3	27	0.09	12830	37.6	82	2.79
4	28	0.089	21316	43.9	85	2.78
5	30	0.089	21415.8	44.09	91	2.84
6	32	0.089	20995	43.09	97	2.78
7	35	0.089	22503	43.94	106	2.83

Table 7.
Training Results for different ANN Architectures of sample X

ANN model no.	No. of Hideen layers	SSE	SSW	NOEP	TNOEP	Mean % Error (test)
1	35	0.277	262289	72	106	5.60
2	45	0.27	182484	82.1	136	5.68
3	50	0.265	212325	94.3	151	5.65
4	65	0.257	262044	107	196	5.62
5	66	0.258	238432	102	199	5.61
6	68	0.257	260221	104	205	5.67
7	69	0.259	212706	98	208	5.68
8	70	0.254	352799	117.3	211	5.73
9	75	0.254	357832	118.3	226	5.69
10	78	0.254	354036	119	235	5.70
12	80	0.254	354193	118.2	217	5.72
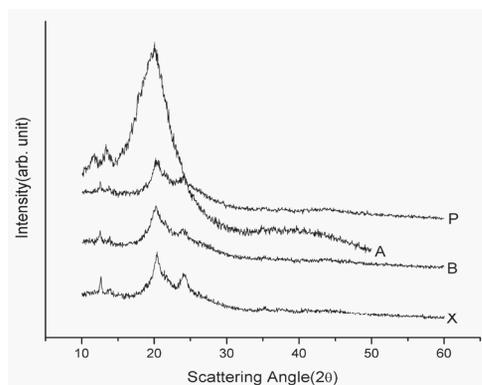
Fig. 7. X-ray diffraction spectra of s-PS/CNF composites

4.2. Training and validation results for the proposed ANFIS and ANN models

This section presents the results obtained on using the proposed ANFIS and ANN models for prediction of intensity from scattering angle in case of samples A, B, X, and P. Figures 8, 9, 10, and 11 exhibit the comparison of the experimental (XRD) and ANN model-predicted intensity values corresponding to sample A, B, P, and X respectively whereas the comparison of the experimental (XRD) and ANFIS model-predicted intensity values corresponding to sample A, B, X, and P are presented through Figures 12, 13, 14, and 15 respectively. The closeness of the experimental and the proposed model-estimated intensity values observed from each of the above-mentioned Figures (Figures 8 – 15) clearly points towards the proposed models' high potential in predicting intensity from scattering angle in XRD of s-PS/CNF composites.
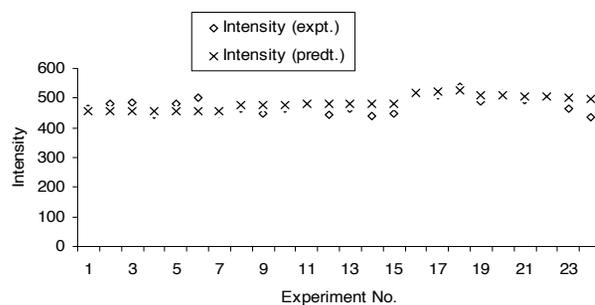
Fig. 8. Comparison of the experimental (XRD) and ANN model-predicted intensity values for sample A
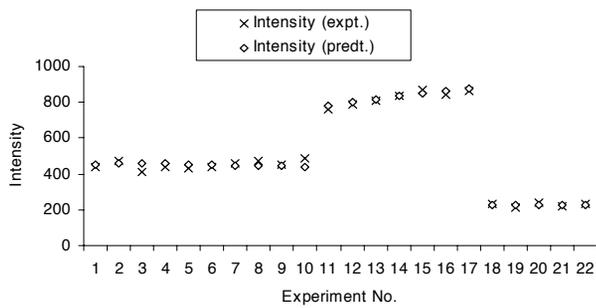
Fig. 9. Comparison of the experimental (XRD) and ANN model-predicted intensity values for sample B
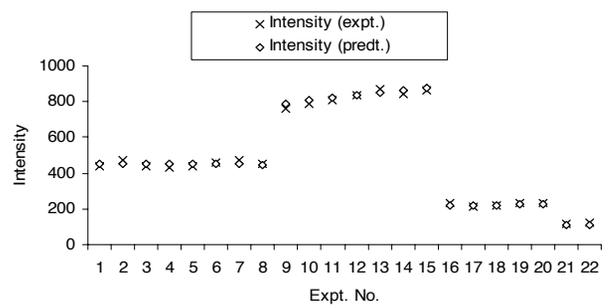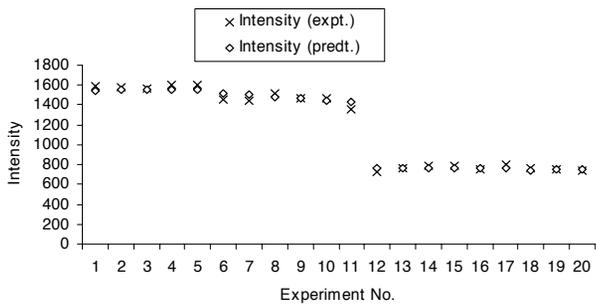
Fig. 10. Comparison of the experimental (XRD) and ANN model-predicted intensity values for sample P
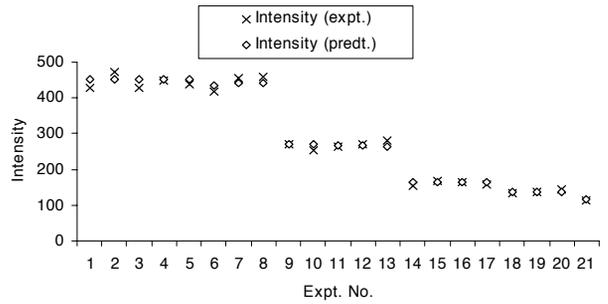
Fig 11. Comparison of the experimental (XRD) and ANN model-predicted intensity values for sample X

Fig. 12. Comparison of the experimental (XRD) and ANFIS model-predicted intensity values for sample A

Fig. 13. Comparison of the experimental (XRD) and ANFIS model-predicted intensity values for sample B
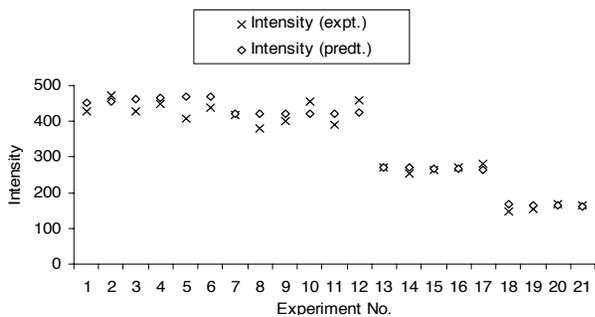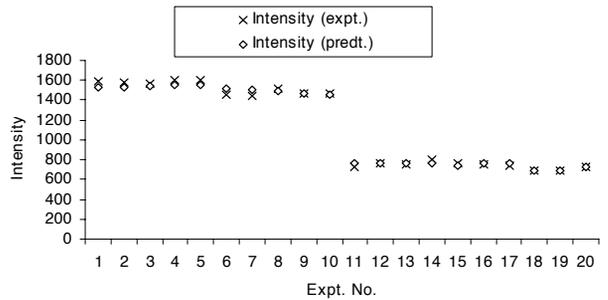
Fig. 14. Comparison of the experimental (XRD) and ANFIS model-predicted intensity values for sample X

Fig. 15. Comparison of the experimental (XRD) and ANFIS model-predicted intensity values for sample P
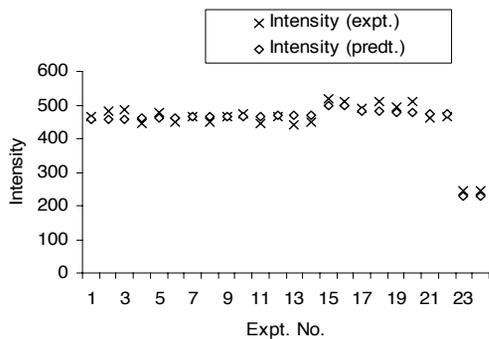
4.3. Comparison between the proposed ANFIS and ANN models

Table 3 carries out a comparison of the proposed ANFIS and ANN models. From Table 3, it is evident that, for each of the composite samples used in this study, the proposed ANFIS model is substantially superior to the corresponding ANN model in terms of mean % error (training) as well as in terms of mean % error (test). However, in case of sample P, it is seen that, the prediction accuracy achieved with the proposed ANFIS model is not very much higher than that achieved with the corresponding ANN model. The above observations are further justified pictorially through Figure 16.
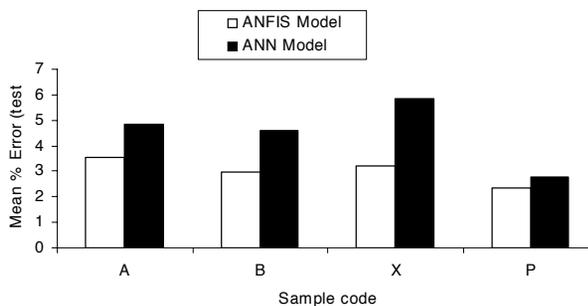
Fig. 16. Comparison of accuracy of the proposed ANFIS and ANN models

5. Conclusions

The results of the investigations carried out in this study is suggestive of the fact that both ANFIS and ANN can be used quite effectively for prediction of intensity from scattering angle values in XRD of s-PS/ CNF composites. The proposed ANFIS and ANN model-predicted intensity values are in very good agreement with the experimental intensity values. However, it is seen that, irrespective of the type of composite sample, the proposed ANFIS models outperform the proposed ANN models in terms of prediction accuracy. Accordingly, it may be concluded that, as far as XRD-based characterization of s-PS/CNF composites is concerned, the quantitative models proposed in this study may act as useful aids.

References

[1] A.R. Bhattacharyya, P. Potschke, H. Liane, D. Fischer, Reactive compatibilization of Melt Mixed PA6/SWNT Composites: mechanical properties and morphology, Macromolecular Chemistry and Physics 206 (2005) 2084-2095.

[2] F.D. Foresee, M.T. Hagan, Gauss-Newton approximation to bayesian regularization, Proceedings of the International Joint Conference "Neural Networks", 1997, 1930-1935.

[3] M.T. Hagan, H.B. Demuth, M.H. Beale, Neural Network Design, MA: PWS Publishing, Boston, 1996.

[4] M.T. Hagan, M. Menhaj, Training feed forward networks with the Marquardt algorithm, IEEE Transactions on Neural Networks 5 (1994) 989-993.

[5] S. Haykin, Neural Network — a comprehensive foundation; a computational approach to learning and machine intelligence, Macmillan, New York, 1994.

[6] M. Hessami, F. Anctil, A.A. Viau, Selection of an Artificial Neural Network Model for the Post-calibration of Weather Radar Rainfall Estimation, Journal of Data Science 2 (2004) 107-124.

[7] S. Jeong, Z. Changchun, L.J. Lee, Synthesis of polystyrene–carbonnanofibers nanocomposite foams, Polymer 46 (2005) 5218-5224.

[8] S.B. Kessler, A.E. Sherif, E. Douglas, D.E. Smith, Incorporating Neural Network Material Models Within Finite Element Analysis for Rheological Behavior Prediction, Transactions of the ASME 129 (2007) 211-214.

[9] A. Kulkarni, Artificial Neural Network for Image Understanding, Van Nostrand Reinhold, New York, 1994.

[10] S. Kumar, T. Rath, R.N. Mahaling, C.S. Reddy, C.K. Das, K.N. Pandey, R.B. Srivastava, S.B. Yadaw, Study on mechanical, morphological and electrical properties of carbon nanofiber/polyetherimide composites, Materials Science and Engineering B 141/1-2 (2007) 61-70.

[11] S. Kumar, T. Rath, R.N. Mahaling, C.K. Das, Processing and characterization of carbonnanofiber/syndiotactic polystyrene composites in the absence and presence of liquid crystalline polymer, Composites: Part A 38/5 (2007) 1304-1317.

[12] Z.C. Lin, C.Y. Liu, Analysis and application of the adaptive neuro-fuzzy inference system in prediction of CMP machining parameters, International Journal of Computer Applications in Technology 17/2 (2003) 80-89.

[13] A. Oonsivilai, M.E. Hawary, Power System Dynamic Load Modeling using Adaptive-Network-Based Fuzzy Inference System, Proceedings of the IEEE Canadian Conference "Electrical and Computer Engineering", Shaw Conference Center, Edmonton, Alberta, Canada, 1999.

[14] T. Ozel, Y. Karpat, Predictive modelling of surface roughness and tool wear in hard turning using regression and neural networks, International Journal of Machine Tools and Manufacture 45 (2005) 467-479.

[15] S. Rajasekharan, S.A.V. Pai, Neural Networks, Fuzzy Logic and Genetic Algorithms, Prentice-Hall, India, 2003.

[16] J.S. Roger, ANFIS: Adaptive-network-based fuzzy inference system, IEEE Transactions on Systems, Man and Cybernetics 23/3 (1993) 665-685.

[17] J.S. Roger, C.T. Sun, Neuro-fuzzy modelling and control, Proceedings of the IEEE 83/3 (1995) 378-406.

[18] K.W. Sandler, S. Pegel, M. Cadek, F. Gojny, E.M. Van, J. Lohmar, Comparative study of melt spun Polyamide12 fibers reinforced with carbon nanotubes and nanofibers, Polymer 45 (2004) 2001-2015.

[19] T. Takagi, M. Sugeno, Derivation of fuzzy control rules from human operator's control actions, Proceedings of the IFAC Symposium "Fuzzy Information, Knowledge Representation and Decision Analysis", Marseilles, France, 1983, 55-60.

[20] E.D. Ubeyli, I. Guler, Adaptive neuro-fuzzy inference system to compute quasi-TEM characteristic parameters of microshield lines with practical cavity sidewall profiles, Neurocomputing 70/1-3 (2006) 296-304.